



Rapid communication

Spiral mechanisms are required to account for summation of complex motion components

Tim S. Meese^{*}, Stephen J. Anderson*Neurosciences Research Institute, School of Life and Health Sciences, Aston University, Birmingham B4 7ET, UK*

Received 3 July 2001; received in revised form 25 February 2002

Abstract

Stimuli from one family of complex motions are defined by their spiral pitch, where cardinal axes represent signed expansion and rotation. Intermediate spirals are represented by intermediate pitches. It is well established that vision contains mechanisms that sum over space and direction to detect these stimuli (Morrone et al., *Nature* 376 (1995) 507) and one possibility is that four cardinal mechanisms encode the entire family. We extended earlier work (Meese & Harris, *Vision Research* 41 (2001) 1901) using sub-threshold summation of random dot kinematograms and a two-interval forced choice technique to investigate this possibility. In our main experiments, the spiral pitch of one component was fixed and that of another was varied in steps of 15° relative to the first. Regardless of whether the fixed component was aligned with cardinal axes or an intermediate spiral, summation to-coherence-threshold between the two components declined as a function of their difference in spiral pitch. Similar experiments showed that none of the following were critical design features or stimulus parameters for our results: superposition of signal dots, limited lifetime dots, the presence of speed gradients, stimulus size or the number of dots. A simplex algorithm was used to fit models containing mechanisms spaced at a pitch of either 90° (cardinal model) or 45° (cardinal + model) and combined using a fourth-root summation rule. For both models, direction half-bandwidth was equated for all mechanisms and was the only free parameter. Only the cardinal + model could account for the full set of results. We conclude that the detection of complex motion in human vision requires both cardinal and spiral mechanisms with a half-bandwidth of approximately 46°. © 2002 Elsevier Science Ltd. All rights reserved.

Keywords: Vision; Optic flow; Random dots; Coherence thresholds; Global motion

1. Introduction

The array of complex retinal motions that occur as an observer moves through a structured environment provides information about the layout of the environment and the observer's position within it (Gibson, 1950; Koenderink, 1986). This has prompted several investigations into how vision might encode complex motions.

Stimuli from one class of complex motions are defined by their spiral pitch, as illustrated in Fig. 1. It is well established that vision contains mechanisms that sum over both space and direction to detect these stimuli (Morrone, Burr, & Vaina, 1995; Harris & Meese, 1996; Burr, Morrone, & Vaina, 1998; Meese & Harris, 2001a), and one intriguing possibility is that just four cardinal mechanisms encode the entire family (Morrone, Burr,

DiPietro, & Stefanelli, 1999; Burr, Badcock, & Ross, 2001). However, there is some evidence from single-cell recordings that, in addition to cardinal units, there are visual neurons in monkey cortex selective for spiral stimuli (Graziano, Andersen, & Snowden, 1994). One useful indicator of the number of mechanisms involved is the direction bandwidth of detecting mechanisms. Bandwidths as broad as $\pm 60^\circ$ are consistent with four cardinal detecting mechanisms alone, but narrower bandwidths require additional intermediate spiral mechanisms to account for psychophysical summation data (Harris & Meese, 1996; Meese & Harris, 2001b). Britten and Newsome (1998) investigated the unidirectional bandwidth of neurons in monkey MT using random dot stimuli close to coherence threshold (to be consistent with psychophysical work) and reported a value of $\pm 45^\circ$. Assuming that these mechanisms provide the input to complex motion mechanisms, then the bandwidths of complex motion mechanisms might be similar to those in MT (Meese & Harris, 2001b),

^{*} Corresponding author. Tel.: +44-121-359361x5421; fax: +44-121-3334220.

E-mail address: t.s.meese@aston.ac.uk (T.S. Meese).

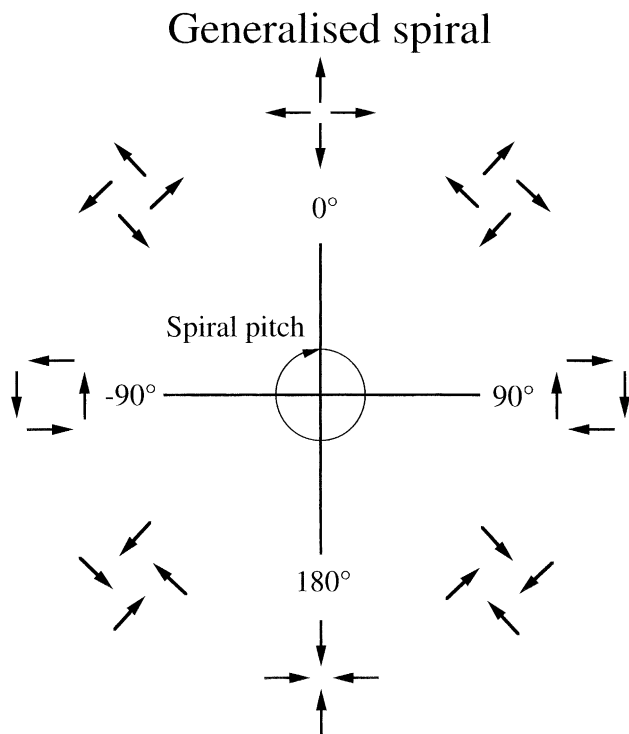


Fig. 1. Two-dimensional representation of the generalised spiral. Spiral pitches of 0° , 90° , 180° and -90° represent expansion, clockwise rotation, contraction, and anticlockwise rotation, respectively. Intermediate spiral pitches represent intermediate spiral stimuli.

suggesting the need for intermediate spiral mechanisms as well as cardinal mechanisms. Indeed, spiral mechanisms with direction bandwidths of $\pm 47^\circ$ were used by Snowden and Milne (1996) in their multi-mechanism model of psychophysical adaptation to complex motion.

Here we extend the subthreshold summation work of Meese and Harris (2001b) to achieve the following two aims. (1) To determine whether generalised spirals (Fig. 1) are detected by cardinal detecting mechanisms or whether intermediate spiral mechanisms are also used. (2) To refine our estimate of direction bandwidth for complex motion mechanisms.

2. Methods

Coherence thresholds (percentage of signal in noise) were measured for random dot patterns of 300 ms duration using interleaved staircases and probit analysis in a two-interval forced choice (2IFC) task using the framstore of a Cambridge Research Systems VSG2/4 graphics board. Signal components were selected from the generalised spiral space shown in Fig. 1.

In Experiment 1, a 5° circular display region (a diameter of 277 pixels) contained approximately 400 bright dots whose luminance was ramped at the boundary and also the centre where there was a small

hole and a stationary fixation point. Sub-pixel accuracy was achieved using the quadratisation technique of Georgeson, Freeman, and Scott-Samuel (1996) which uses a square of four pixels to represent each stimulus dot. Movies consisted of sequences of four images each displayed for nine frames on a 120 Hz monitor. Stimuli contained a 10% speed gradient meaning that each dot travelled a distance of $d/10$, where d is the distance of the mid-point of its trajectory from the centre of the display. This gave dot speeds of $0.83^\circ \text{ s}^{-1}$ towards the outer edge of the display. For the expansion stimulus, this simulated an approaching surface at a distance of 2.5 m moving at a walking speed of about 2.76 km/h. These provided a striking impression of brief sequences of spatial texture characterised by smooth global motion.

In preliminary detection experiments, observers detected the presence of individual components whose level (percentage of signal dots) was controlled by one of six randomly interleaved staircases. These estimates were used to set the mechanism gains in models of the data. In subsequent summation experiments, compound stimuli contained a signal made from pairs of components referred to as component A and component B. Unlike previous work (Meese & Harris, 2001a,b), we did not use the estimates of individual component sensitivity to weight the component levels in the compound stimuli, but set the level of component A equal to that of component B. An experimental session consisted of a series of 2IFC trials controlled by seven randomly interleaved staircases, where the pitch of component A was fixed at either -45° , 0° or $+45^\circ$ (see Fig. 1). The pitch of signal B was different for each staircase and varied in 15° steps from 0° to 90° relative to the pitch of component B.

In Experiment 2, the summation experiment was repeated but the two signal components were randomly allocated to alternate display sectors (from a total of 8) on each trial. In Experiment 3, both detection and summation experiments were repeated with the following modifications: (i) the 10% speed gradient was removed; (ii) all dots (both signal and noise) travelled a distance of 0.25° (a constant speed of $0.83^\circ \text{ s}^{-1}$); (iii) the viewing distance was halved from 114 to 57 cm to double the display diameter to 10° and (iv) the number of dots was reduced by a factor of 4.

In Experiment 4, only pairs of orthogonal complex motions were investigated, and the normalisation technique of Meese and Harris (2001a,b) was used. This involved a preliminary stage in which thresholds for the two individual components were estimated and weighted accordingly in a compound stimulus whose threshold was measured in a second stage. Viewing distance was 114 cm, display diameter was 10° , there were approximately 400 dots, stimulus duration was 350 ms, stimulus speed was either 3 or 6° s^{-1} , and the movies consisted of

6 or 7 image frames. All dots had limited life-times and on each image frame, half of them ‘died’ and the other half were ‘reborn’. On each ‘rebirth’, the position of the midpoint of each dot trajectory (between successive image frames while it was ‘alive’) was allocated randomly across the entire display region, meaning that the average image statistics for each image frame were identical.

In Experiments 1–3 and Experiment 4, thresholds are the geometric means of at least six and four estimates respectively, and error bars show ± 1 SE. Data were gathered for two observers, both of whom had corrected-to-normal visual acuity and substantial preliminary practice with the stimuli.

A more detailed description of our methods and stimuli and a description of the equipment can be found in Meese and Harris (2001a,b).

3. Results: Experiment 1

3.1. Coherence thresholds

Fig. 2A and B shows the coherence thresholds for the two authors as a function of spiral pitch. Consistent with previous findings (e.g. Morrone et al., 1999; Burr et al., 2001), there are differences in detail between the observers. Nevertheless, while the effects are small, there is a tendency for sensitivity to be greater for cardinal directions than for intermediate spirals; the three and two most sensitive directions are cardinal for SJA and TSM, respectively. We also note that in general, the coherence thresholds are a little higher than those reported elsewhere (e.g. Scase, Braddick, & Raymond, 1996; Meese & Harris, 2001a). This is probably due to stimulus uncertainty which would have been higher here because of the stimulus interleaving.

3.2. Summation

Fig. 2C and D shows summation data for a pair of stimulus components where one of the components (A) was always expansion (pitch = 0°) and the pitch of the other (B) is given by the abscissa. For both observers (different panels), summation declines as a function of the pitch of the second component. The curves are predictions for models (see later for further details) which include either cardinal detecting mechanisms alone (cardinal model; dashed curve) or cardinal mechanisms plus intermediate spiral mechanisms (cardinal + model; solid curve). Both models provide acceptable fits to the data (see root mean square errors (RMS) in figure insets).

In Fig. 2E and F, component A was always a spiral (pitch = -45°), though the pattern of summation is very similar to when it was expansion. In this case, however,

only the cardinal + model provides a good fit to the data. The cardinal model considerably overestimates the amount of summation for several different values of pitch.

4. Results: Experiment 2

In Experiment 2, the two components in the compound stimulus were placed in alternate sectors so as to avoid local interactions between signal dots either on the display monitor or within early unidirectional motion mechanisms. Fig. 3A and B shows results where component A was expansion and spiral, respectively. The results replicate those of Experiment 1: summation declines as the pitch of component B increases, regardless of the pitch of component A, and the full data set are well fit only by the cardinal + model. We conclude that sectorizing the two signal components was not an important manipulation (also see Meese & Harris, 2001a).

5. Results: Experiment 3

Contrary to our findings in Experiments 1 and 2, Burr et al. (2001) have recently reported substantial summation for orthogonal spiral stimuli, suggesting that both components were being summed within a single cardinal detecting mechanism. To investigate whether these differences might be in some way related to subtle differences in the stimuli used in the two studies, we repeated our experiment using stimuli that more closely matched those of Burr et al. Specifically, we removed the speed gradient and matched the size of the stimulus (10°) and the number of dots (100) to those used by Burr et al. The experiment was also performed with the spirals balanced around expansion and rotation. In both cases (Figs. 4 and 5) the pattern of results was similar to before, though in Fig. 5 the distinction between model predictions was less than in earlier experiments. This was due to the setting of mechanism gains according to the pattern of detection data (Fig. 5A): for the cardinal model an ‘off-stimulus’ mechanism (the expansion mechanism) made a substantial contribution to the detection of component A but contributed little to the detection of component B over much of its range. Nevertheless, the data are best captured by the cardinal + model, mainly due to the better fit of this model when the stimulus components were orthogonal (rightmost data point in Fig. 5B).

We conclude that speed gradients, dot number, stimulus size and the axis around which the spiral components were balanced were not critical parameters for our results.

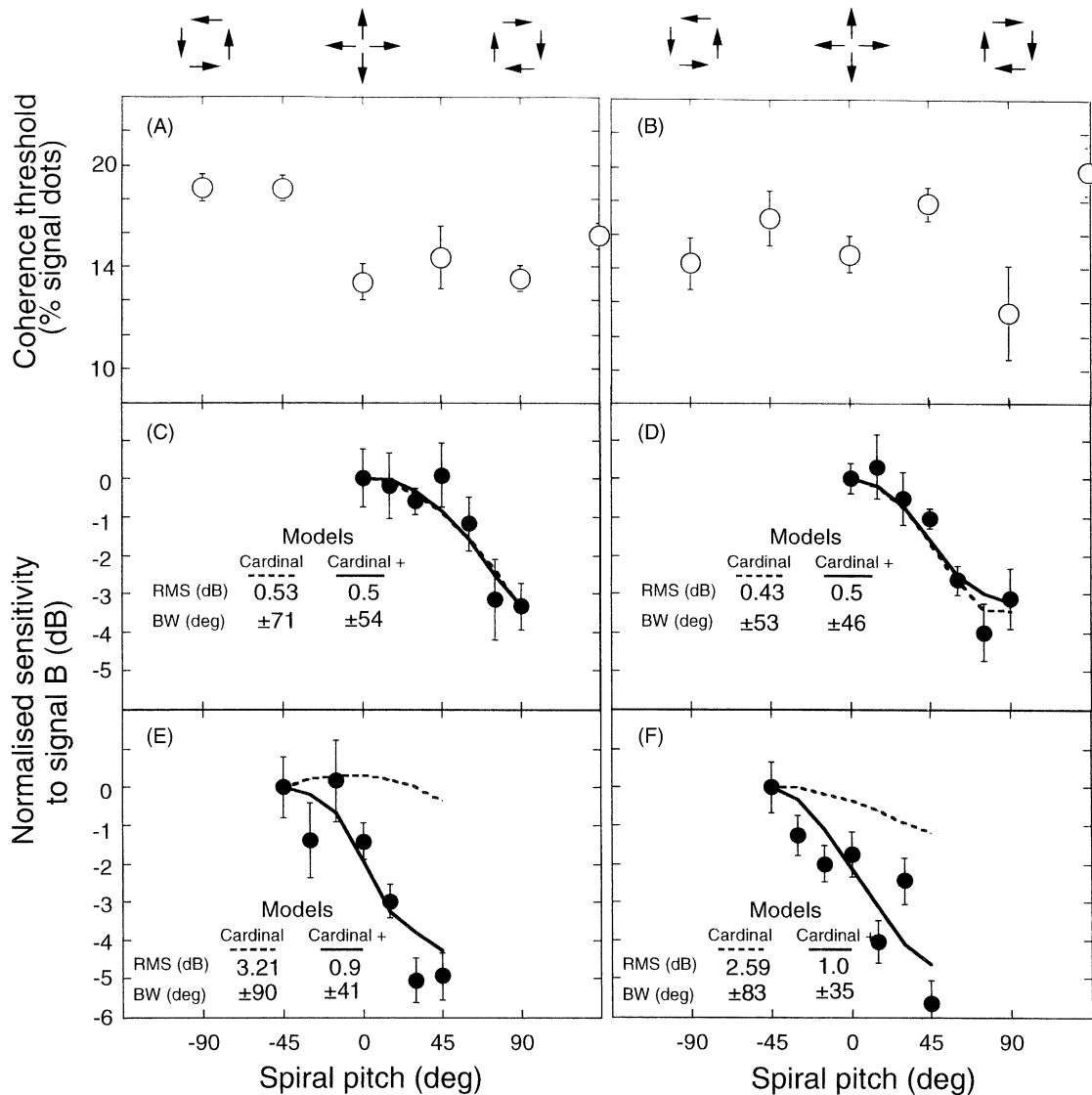


Fig. 2. Results from Experiment 1. Coherence thresholds and summation for generalised spiral stimuli as a function of spiral pitch for TSM (A, C, E) and SJA (B, D, F). A, B: single component coherence thresholds. The range of spiral pitches investigated were those necessary for the model predictions for the summation data (six stimuli for each observer). Note the log scale for the ordinate. C, D: summation results, where component A was always expansion (pitch = 0°) and the pitch of component B is given by the abscissa. Sensitivity to component B ($20\log[1/T]$, where T is the coherence threshold for component B) is normalised to that found when both components were the same (6dB = a factor of two). The curves are for models containing either cardinal detecting mechanisms alone (dashed), or cardinal plus intermediate spiral mechanisms (solid). Direction bandwidth (BW) of the detecting mechanisms was the only free parameter in the models and the estimate performed by the curve fitting procedure is shown in the inset along with the root mean square (RMS) error of the fit. E, F: summation results where component A was always anticlockwise spiral (pitch = -45°) and the pitch of component B is given by the abscissa. The curves are for the same two models as in (C, D).

6. Results: Experiment 4

Experiments 1–3 have two limitations. First, unlimited life-time dots were used which means that, in principle, static image cues such as dot density might have served as a cue for detection, at least for those signals containing a component of expansion. (We note, however, that bunching of dots was not evident in our stimuli; see Meese & Harris (2001a) for a control experiment.) Second, although the dot speeds are within the range of speeds to which cortical cells respond (e.g.

Maunsell & van Essen, 1983), they are at the lower end, and are slower than dot speeds used in psychophysical experiments elsewhere (e.g. Burr et al., 2001). To counter these limitations, in our final experiment limited life-time dots were used in displays where dots travelled at either 3 or 6° s⁻¹.

The use of a normalization technique (see Section 2) allows summation ratios to be plotted directly and these are shown in Fig. 6 for configurations in which the component pairs were orthogonal (see figure caption for details). The dashed and solid lines are the predictions

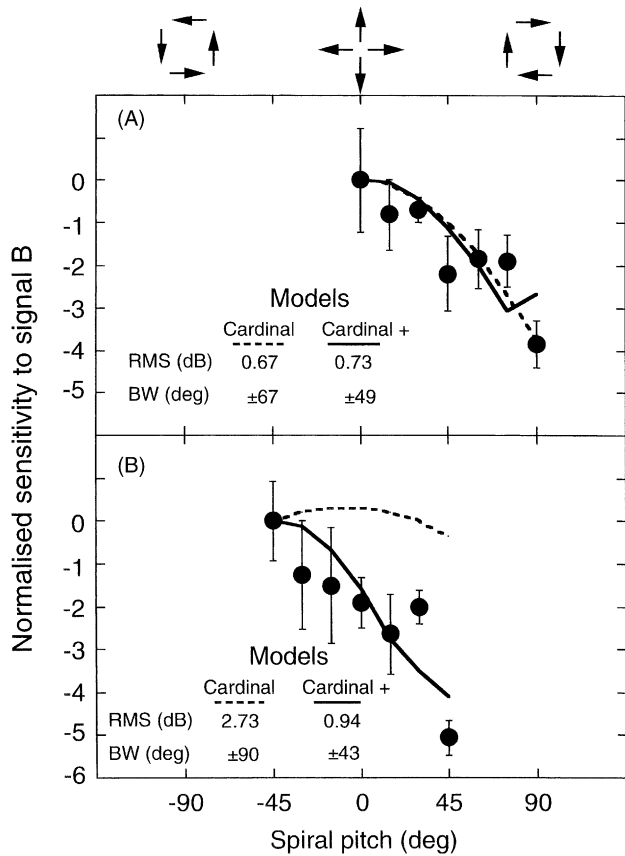


Fig. 3. Summation results from Experiment 2 (TSM), where the two different components were placed in alternate sectors. Component A was expansion (pitch = 0°) in (A) and anticlockwise spiral (pitch = -45°) in (B). The pitch of component B is given by the abscissa.

for the cardinal model and the cardinal + model, respectively. The greatest difference in the model predictions is for the spiral conditions. For the cardinal + model, summation was overestimated by only 0.89 dB but for the cardinal model, by 3.4 dB (results averaged over both observers and both speeds). In the cardinal + model, summation is mainly due to probability summation between detecting mechanisms, and the difference of 0.89 dB between data and model might reflect a failure of observers to monitor all relevant mechanisms. (Similar mismatches between the data and model can be seen for orthogonal component conditions in the earlier experiments.) In the cardinal model, the difference between data and model is more substantial and, furthermore, cannot easily be dismissed because the summation is mainly due to linear summation within the most sensitive detecting mechanism.

Another difference between the models is that the cardinal + model predicts the same level of performance for all stimulus conditions, whereas the cardinal model predicts that summation should be less (by more than 3 dB) for the expansion/rotation conditions than for the spiral conditions. The largest difference in the data was

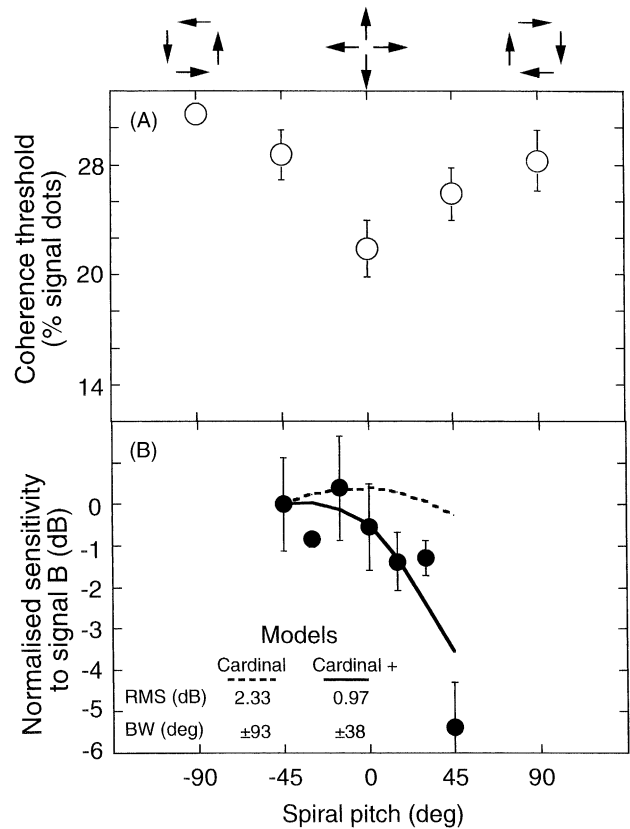


Fig. 4. Results from Experiment 3 (TSM), where stimulus conditions were more similar to those used by Burr et al. (2001). The display diameter was increased to 10° and the number of stimulus dots was decreased to 100. The detection data in (A) were used to set the gains of the model mechanisms for the summation data in (B) where signal A was always anticlockwise spiral (spiral pitch = -45°) and the pitch of component B is given by the abscissa.

for a speed of 3° s⁻¹ (SJA), though it was less than half that predicted by the cardinal model. For all remaining conditions there was little or no difference in summation between spiral and expansion/rotation conditions, in agreement with the cardinal + model.

We conclude that our earlier results are not peculiar to particular dot speeds or the use of unlimited life-time displays.

7. Models

For Experiments 1–3, two models were fit to each summation data set: one containing four cardinal mechanisms (the cardinal model) and the other containing four cardinal plus four intermediate spiral mechanisms (the cardinal + model), as illustrated by the eight stimulus tokens in Fig. 1. The direction tuning function of the global detecting mechanisms had the shape of a positive lobe of a cosine function and its bandwidth (the only free parameter) was controlled by a simplex algorithm (Press, Flannery, Teukolsky, & Vetterling, 1989)

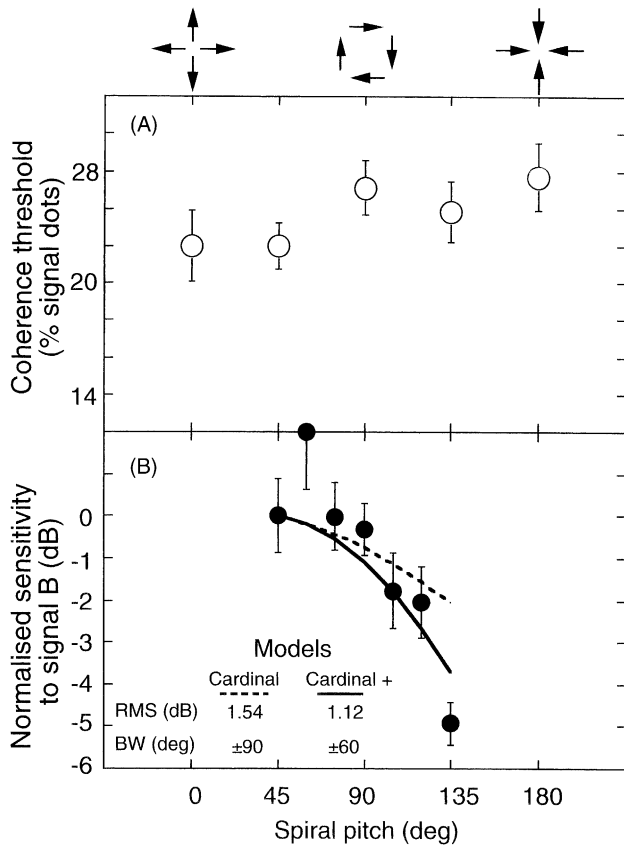


Fig. 5. As Fig. 4, except the experimental conditions were balanced around rotation (pitch = 90°) instead of expansion (pitch = 0°). Note that in (B), the difference in the two model predictions (different curves) is less than in other figures. This is due to the pattern of the detection data (A) which was different from before (e.g. Fig. 4), and which led to a different pattern of mechanism gains being used.

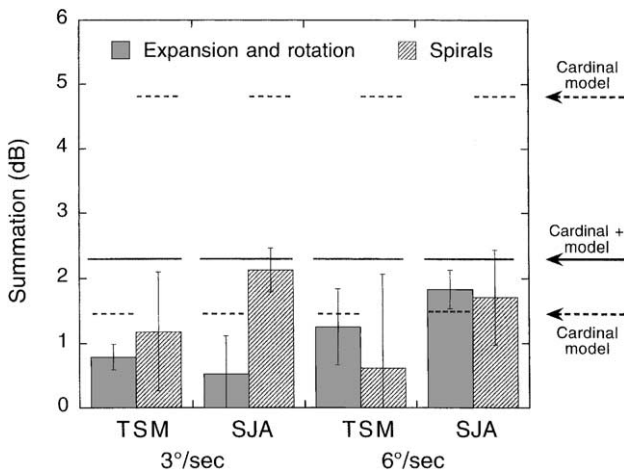


Fig. 6. Results from Experiment 4 for TSM and SJA. Summation ratios ($20 \log[T^*/T]$, where T^* is the coherence threshold for a component when measured alone and T is the coherence threshold for that same component in the compound stimulus) for two observers, two speeds, and component pairs of expansion (pitch = 0°) and rotation (pitch = 90°) and a pair of spirals balanced around rotation (pitch = 45° and 135°). The dashed and solid lines show predictions for the cardinal and cardinal + models, respectively.

that optimised the RMS error of the fit. Probability summation was assumed between all detecting mechanisms in the summation experiments and was simulated using a Minkowski metric (Graham, 1989) with the summation exponent set to 4 (e.g. Quick, 1974; Meese & Williams, 2000; Tyler & Chen, 2000). Mechanism gains were equated with the sensitivities measured in the detection experiments (i.e. they were the reciprocals of coherence thresholds for the appropriate components) and mechanisms were assumed to be linear. These estimates of gain did not take into account possible small effects of probability summation from multiple mechanisms but under the circumstances of the present paper were fair approximations. For example, only relative mechanism gain can affect model performance: multiplying the entire family of gains by a constant (>0) does not alter the predictions. Moreover, we found that the general pattern of model predictions was much the same when the mechanism gains were equated, indicating that the predictions are robust against small misestimates of relative gain.

Model predictions are plotted in each of the summation figures and the insets show the RMS error (in dB) and the estimate of bandwidth (half-width at half-height) for each of the two models. When the fixed component was expansion, both models provided a good account of the data, but when the fixed component was a spiral, the cardinal + model always provided a better fit (lower RMS error), often substantially so. In all cases, bandwidth estimates were broader for the cardinal model (average = 64°) than for the cardinal + model (average = 46°).

An important feature of the summation figures is that the model predictions (and the data) have been normalised to the sensitivity to component A. This explains why less summation is predicted when component A is expansion and component B is spiral (e.g. left most data point in Fig. 2C) than when component A is spiral and component B is expansion (e.g. left most data point in Fig. 2E). In the first case, summation is relative to expansion sensitivity and in the second case, it is relative to spiral sensitivity. This was not a feature of our earlier modelling (Meese & Harris, 2001a,b; Fig. 4A) where component normalisation was performed by weighted contributions in the compound stimulus.

In Experiment 4, models were approximations in which the normalisation of stimulus components was assumed to be equivalent to using components of equal weights and mechanisms with equal gains. The models were otherwise the same as described above but with direction bandwidths fixed at ±46° for the cardinal + model (see above), and ±60° for the cardinal model (Morrone et al., 1999). If neural mechanism gains were in fact less for spiral mechanisms than for cardinal mechanisms (as suggested by the data from Experiment 1), then for the cardinal + model this approximation slightly overesti-

mates summation between expansion and rotation, and slightly underestimates summation between the spirals.

8. Discussion

Our complete data set is well described by the cardinal + model but poorly fit by the cardinal model. This provides evidence for spiral detecting mechanisms, consistent with the adaptation study of Snowden and Milne (1996) and the single-cell recordings in monkey area MSTd performed by Graziano et al. (1994). Our results also allow us to refine earlier estimates of direction bandwidth for complex motion mechanisms (Meese & Harris, 2001b). The average across all of the cardinal + model fits is $\pm 46^\circ$ ($SD = 8^\circ$) which is within the range previously identified by Meese and Harris (2001b). This is remarkably similar to the value of $\pm 45^\circ$ estimated by Britten and Newsome (1998) for neurons in monkey area MT and the value of $\pm 47^\circ$ used by Snowden and Milne (1996) in their model of adaptation to complex motion. Note that all of these estimates are narrower than those estimated using only cardinal mechanisms (see Figs. 3 and 5) and narrower than that which can achieve perfect positional invariance ($\pm 60^\circ$; Zhang, Sereno, & Sereno, 1993).

In sum, we conclude that the detection of generalised spiral stimuli cannot be accomplished by cardinal mechanisms alone. Rather, a minimum of eight mechanisms with direction bandwidths around $\pm 45^\circ$ are required. This is at odds with the work of Burr et al. (2001) who measured summation only for orthogonal stimulus components, as in our Experiment 4 and equivalent to the condition represented by the right most data point in our main summation figures. Contrary to our own results, when the orthogonal stimuli were spirals, Burr et al. found substantial summation, suggesting that detection of these stimuli was accomplished by cardinal mechanisms. The main differences between our Experiment 3 and that of Burr et al. were: (1) limited life-time dots used by Burr et al., (2) slower speeds used here (0.83°s^{-1} as opposed to 6.0°s^{-1}), (3) sectorization of the display by Burr et al., (4) a 2IFC detection paradigm used here and a single interval discrimination paradigm used by Burr et al. However, in Experiment 2, we used sectorized displays and in Experiment 4, we used faster stimulus speeds (3.0° and 6.0°s^{-1}) and limited life-time dots, but in no case was there a change in our main finding. This suggests that the important difference might be the investigative methodologies used in the two studies. In our experiments, observers reported which of two temporal intervals contained structured motion. Thus, the task demands were the same for all conditions. In Burr et al.'s (2001) experiments, observers reported in which direction a stimulus pattern moved (e.g. clockwise or

anticlockwise). Thus, in their summation experiments, observers had to keep track of two pairs of directions. For example, expansion or anticlockwise rotation might be associated with one response button and contraction and clockwise rotation might be associated with another. This might be straightforward for the example just considered but possibly more complicated when the orthogonal stimuli were spirals whose appearances are more difficult to intuit. In such cases, observers might simplify the cognitive demand by internally summarising orthogonal spiral pairs by their intermediate motion; clockwise and anticlockwise spirals with pitches of -45° and 45° becoming expansion for example. In other words, one possible interpretation of the cardinal behaviour found by Burr et al. is that it represents an anisotropy in observer strategy or attention rather than properties of sensory mechanisms. On the other hand, we note that this account cannot be applied to the results of a masking experiment reported in the same paper where, in a 2IFC design, thresholds for spiral test stimuli (containing 25 signal and noise dots) were higher for cardinal masks (containing 75 dots) than they were for spiral masks (see Fig. 4 in Burr et al., 2001).

Finally, we note that although it was necessary for us to include spiral detecting mechanisms in order to account for our full data set, the gains of these mechanisms were typically lower than those for cardinal mechanisms (see Fig. 2), consistent with previous results where a distinct anisotropy for generalised spirals was reported (Morrone et al., 1999). Indeed, although the results of Burr et al. (2001) suggest cardinal mechanisms, the authors did accept that there may well exist neurons with intermediate spiral tuning that are less sensitive (or fewer in number) than those tuned to cardinal axes. This suggestion sits comfortably with a recent report where Glass patterns were used to investigate the detection of complex form (Seu & Ferrera, 2001). Although sensitivities to cardinal patterns with concentric and radial forms were found to be higher than to intermediate spiral forms, the authors concluded that intermediate spiral mechanisms (with lower gains) were necessary to account for their data.

Acknowledgement

This work was first presented in abstract form at the first meeting of the Vision Sciences Society (VSS) in Sarasota, USA, May 4–8, 2001.

References

- Britten, K. H., & Newsome, W. T. (1998). Tuning bandwidths for near-threshold stimuli in area MT. *Journal of Neurophysiology*, *80*, 762–770.

- Burr, D. C., Badcock, D. R., & Ross, J. (2001). Cardinal axes for radial and circular motion, revealed by summation and by masking. *Vision Research*, *41*, 473–481.
- Burr, D. C., Morrone, M. C., & Vaina, L. M. (1998). Large receptive fields for optic flow detection in humans. *Vision Research*, *38*, 1731–1743.
- Georgeson, M. A., Freeman, T. C. A., & Scott-Samuel, N. E. (1996). Sub-pixel accuracy: Psychophysical validation of an algorithm for fine positioning and movement of dots on visual displays. *Vision Research*, *36*, 605–612.
- Gibson, J. J. (1950). *The perception of the visual world*. Boston: Houghton-Mifflin.
- Graham, N. (1989). *Visual pattern analyzers*. Oxford: Oxford University Press.
- Graziano, M. S. A., Andersen, R. A., & Snowden, R. J. (1994). Tuning of MST neurons to spiral motions. *The Journal of Neuroscience*, *14*, 54–67.
- Harris, M. G., & Meese, T. S. (1996). Human vision employs pooling mechanisms for rotation, expansion and deformation components of optic flow [ECP Abstract]. *Perception*, *25*(supp.), 129.
- Koenderink, J. J. (1986). Optic flow. *Vision Research*, *26*, 161–179.
- Maunsell, J. H. R., & van Essen, D. C. (1983). Functional properties of neurons in middle temporal visual area of the macaque monkey. I. Selectivity for stimulus direction, speed and orientation. *Journal of Neurophysiology*, *49*, 1127–1147.
- Meese, T. S., & Harris, M. G. (2001a). Independent detectors for orthogonal components of complex motion. *Perception*, *30*, 1189–1202.
- Meese, T. S., & Harris, M. G. (2001b). Broad direction bandwidths for complex motion mechanisms. *Vision Research*, *41*, 1901–1914.
- Meese, T. S., & Williams, C. B. (2000). Probability summation for multiple patches of luminance modulation. *Vision Research*, *40*, 2101–2113.
- Morrone, M. C., Burr, D. C., & Vaina, L. M. (1995). Two stages of visual processing for radial and circular motion. *Nature*, *376*, 507–509.
- Morrone, M. C., Burr, D. C., DiPietro, S., & Stefanelli, M. (1999). Cardinal directions for optic flow. *Current Biology*, *9*, 763–766.
- Press, W. H., Flannery, B. P., Teukolsky, S. A., & Vetterling, W. T. (1989). *Numerical recipes in Pascal: the art of scientific computing*. Cambridge: Cambridge University Press.
- Quick, R. F. (1974). A vector-magnitude model of contrast detection. *Kybernetik*, *16*, 65–67.
- Scase, M. O., Braddick, O. J., & Raymond, J. E. (1996). What is noise for the motion system? *Vision Research*, *36*, 2579–2586.
- Seu, L., & Ferrera, V. P. (2001). Detection thresholds for spiral glass patterns. *Vision Research*, *41*, 3785–3790.
- Snowden, R. J., & Milne, A. B. (1996). The effects of adapting to complex motions: position invariance and tuning to spiral motions. *Journal of Cognitive Neuroscience*, *8*, 435–452.
- Tyler, C. W., & Chen, C.-C. (2000). Signal detection theory in the 2AFC paradigm: Attention, channel uncertainty and probability summation. *Vision Research*, *40*, 3121–3144.
- Zhang, K., Sereno, M. I., & Sereno, M. E. (1993). Emergence of position-independent detectors of sense of rotation and dilation with Hebbian learning: an analysis. *Neural Computation*, *5*, 597–612.